

Calibration of particle detectors for secondary cosmic rays using gamma-ray beams from thunderclouds



A. Chilingarian^{a,*}, S. Chilingaryan^{a,b}, G. Hovsepyan^a

^a Yerevan Physics Institute, Alikhanian Brothers 2, Yerevan 36, Armenia

^b IPE, Karlsruhe Institute of Technology, Postfach 3640, 76021 Karlsruhe, Germany

ARTICLE INFO

Article history:

Received 11 August 2014

Received in revised form 29 March 2015

Accepted 30 March 2015

Available online 4 April 2015

Keywords:

Particle detectors

Atmospheric electricity

Thunderstorm Ground Enhancements

ABSTRACT

After observation of hundreds of Thunderstorm Ground Enhancements (TGEs) we measure energy spectra of particles originated in clouds and directed towards Earth. We use these “beams” for calibration of cosmic ray detectors located beneath the clouds at an altitude of 3200 m at Mount Aragats in Armenia. The calibrations of particle detectors with fluxes of TGE gamma rays are in good agreement with simulation results and allow estimation of the energy thresholds and efficiencies of numerous particle detectors used for studying galactic and solar cosmic rays.

© 2015 Elsevier B.V. All rights reserved.

1. Introduction

Networks of particle detectors located on the Earth's surface continuously measure the incident flux of cosmic rays. These networks cover areas up to thousands of square kilometers and are investigating ultrahigh energy cosmic rays (UHECR) which have been accelerated during the most violent explosions in the Universe. Smaller surface arrays of a few square kilometers or less are detecting mostly galactic cosmic rays (GCR) to locate their sources and identify the acceleration mechanisms. Worldwide networks of particle detectors of several square meters area detect solar cosmic rays (SCR) with the aim of understanding solar accelerators and solar terrestrial connections, in particular space weather phenomena. Last but not least, small size spectrometers at atomic power stations monitor radioactive isotopes escaping to the atmosphere. Interestingly, all these four types of detectors are used for research in the emerging field of high-energy physics in the atmosphere, measuring particle fluxes from thunderclouds [9,10].

The Aragats Space Environmental Center (ASEC, [2]) consists of different particle detectors registering almost all types of the secondary cosmic rays. ASEC is operated by the Cosmic Ray Division (CRD) of the Yerevan Physics Institute and is located at altitudes of 2000 and 3200 m, respectively, on the slopes of Mt. Aragats in Armenia. Research at ASEC includes registration of Extensive Air Showers (EAS) with large particle detector arrays, investigation of

solar acceleration mechanisms, monitoring of space weather and observations of high-energy particles from thunderclouds. Nearly 500 particle detectors (mostly plastic scintillators read out with photomultipliers) are sending data every minute (or second) to the CRD headquarters in Yerevan. In addition to particle detectors, ASEC includes facilities measuring electric and geomagnetic fields, lightning occurrences and locations, broadband radio emission, a variety of meteorological parameters, and optical images of clouds and lightnings.

Dealing with ultra-high energy, galactic and solar cosmic rays, one of the most important tasks is the determination of the detector response. Usually it is estimated with the help of the GEANT detector simulation package [1], a standard tool in high-energy and astroparticle physics. However, it is important to perform calibration experiments with particle beams, too, with the aim to validate the calculated energy threshold, the response to different types of particles and the efficiency of their detection. While calibration with artificial particle beams is standard practice in accelerator experiments, there are only few attempts to calibrate cosmic ray surface detectors with particle beams. These attempts are related to the calibration of fluorescence detectors with lidars or linear accelerators. For instance, the Telescope Array has used an electron linac with beam pulses of one microsecond length and 10^9 electrons of 40 MeV, injected vertically upwards into the atmosphere to calibrate its fluorescence detectors. The calculated energy deposit of the beam in the atmosphere together with the fluorescence yield per deposited energy gives the number of photons expected at the telescope, which can be compared with the measured number of photons [12].

* Corresponding author.

E-mail address: chili@aragats.am (A. Chilingarian).

At Mt. Aragats, Thunderstorm Ground Enhancements (fluxes of electrons, gamma rays and neutrons from thunderclouds, [3,4]) are usual phenomena, due to frequent storms, especially in spring and autumn. Large fluxes of the registered gamma rays allow precise recovery of the shape (usually a power law) and the slope of the gamma-ray spectrum. A network of large NaI crystals recently installed at ASEC opens new opportunities to use the measured beams of gamma rays *a posteriori* for the determination of the detector response. On a very small energy scale (the energies of electrons accelerated in thunderclouds do not exceed 50 MeV and gamma rays are below 100 MeV), this can be seen as the realization of an old vision of cosmic ray physicists: to arrange a particle accelerator in the atmosphere just above the EAS detectors. The proposed methodology allows estimation and monitoring of one of the important parameters of particle detectors, their energy threshold. We use the gamma ray “beams” to calculate the detector response of various particle detectors located beneath the thundercloud. We demonstrate, how the energy threshold of plastic scintillation counters to MeV gamma rays from the atmosphere can be calibrated with the help of neighboring NaI counters. The basic steps are the following:

- We perform a continuous monitoring of the secondary cosmic ray fluxes with the ASEC particle detectors and spectrometers.
- We select a data sample of ionizing atmospheric radiation from the thunderclouds (TGE events) where we know that gamma rays contribute a significant part.
- We measure the energy spectrum of the TGE events with the help of the network of large NaI spectrometers.
- We observe a power law spectrum between 4 and 100 MeV, which we assume to extend below the threshold for the NaI configuration.
- We select TGE events for which the electron/gamma ratio in the plastic scintillators should be no larger than 1–2%.
- We compare the count rates of plastic scintillators of various types and sizes to the integral energy spectrum recovered by the network of NaI crystal. Assuming a pure power law between 0.5 and 10 MeV and normalizing the scintillator apertures to the NaI aperture, the counting rate can be translated to an integral energy spectrum J_E (with $E > E_{\text{threshold}}$).

2. Short description of some of the particle detectors

The NaI network consists of five NaI crystal scintillators, each in a sealed 1-mm-thick aluminum housing. The hygroscopic NaI crystal is protected against humidity by 0.5 cm thick sheets of magnesium, with a transparent window directed to the photo-cathode of the photomultiplier tube PM-49; see Fig. 1. The large photocathode of PM-49 (15-cm diameter) provides good light collection. The range of spectral sensitivity of PM-49 is 300–850 nm, which covers the emission spectrum of NaI(Tl). The sensitive area of each NaI crystal is $\sim 0.032 \text{ m}^2$; the total area of the five crystals is $\sim 0.16 \text{ m}^2$; the efficiency to detect a gamma ray is $\sim 80\%$.

SEVAN (Space Environmental Viewing and Analysis Network) is a network of particle detectors aimed to improve research of particle acceleration in the vicinity of the Sun as well as solar terrestrial relations. The modules of the SEVAN network (Fig. 2) simultaneously measure the flux and variations of three species of secondary cosmic rays to explore solar modulation effects. Two identical assemblies of $100 \times 100 \times 5 \text{ cm}^3$ plastic scintillators and lead absorbers sandwich a smaller scintillator assembly of $50 \times 50 \times 20 \text{ cm}^3$.

The new generation of ASEC detectors comprises 1 and 3 cm thick molded plastic scintillators arranged in stacks (STAND1 detector, Fig. 3) and in cubical structures (CUBE detector, Fig. 4),

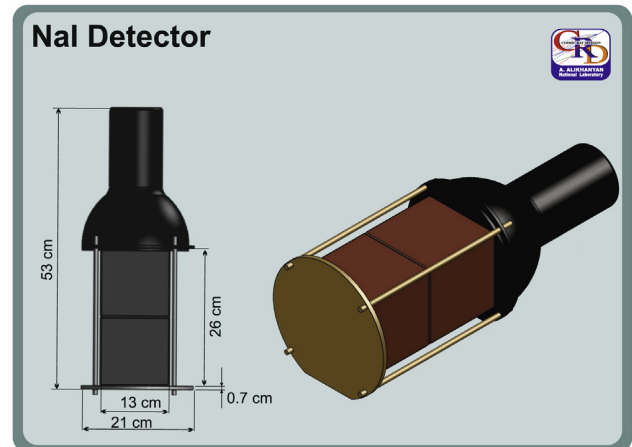


Fig. 1. Configuration of the NaI(Tl) spectrometer.

light from the scintillators is re-radiated by wavelength shifting optical fibers at larger wavelengths and propagates to photomultipliers of the type PM-115M. The DAQ electronics stores all configurations of the signals in the detector channels. If a signal is detected only in the upper scintillator, we register the code “100”. The code “010” corresponds to a signal only in the middle scintillator, and so on.

The Cube detector (Fig. 4) consists of six 1-cm thick plastic scintillators of the same type as used in the STAND1 detector. They surround two stacked 20 cm thick scintillators and can veto charged particles crossing the thick inner scintillators. They allow enrichment of the data sample with neutral particles and in particular estimating the fraction of electrons in the mixed electron and gamma ray flux. Furthermore, there other detectors used which are not described here. The detailed detector charts with all sizes are available from the WEB site of the Cosmic Ray Division of Yerevan Physics Institute: <http://crd.yerphi.am/>.

3. Recovering gamma ray spectra: the TGE detected on 27 May 2014

The electron flux in the atmosphere is much more attenuated than the gamma ray flux. Therefore, most of the particles registered by the surface detectors are gamma rays. However, sometimes, when a thundercloud is very low above the Earth's surface, the fraction of electrons in the total flux can be sizeable (see details in [6]). For calibration purposes we select from the observed TGEs those with a fraction of electrons not exceeding 1–2% of the total flux. We demonstrate the techniques to select approximately “pure gamma ray” TGEs with the help of a double peaked TGE detected on May 27, 2014.

On May 27, 8:40 UTC, the electric mill located at the Aragats research station recorded a large disturbance in the near-surface electric field related to the arrival of a large thundercloud, see Fig. 5. Ten minutes after a positive boost of the electric field (reaching a maximal value of +15 kV/m), at 8:50 the electric field abruptly changed the polarity to a field strength of -15 kV/m . The decrease of the solar radiation from 1200 to 100 W/m^2 during the TGE confirms the presence of the dense cloud just above the detectors. The high humidity of 88–97% allows the development of a Lower Positively Charged Region (LPCR) formed by the polarized micro-droplets of water [11]. Two oppositely charged layers – the positively charged LPCR and the negatively charged layer above – in the thundercloud formed a lower dipole accelerating electrons downward (see for details [8]).

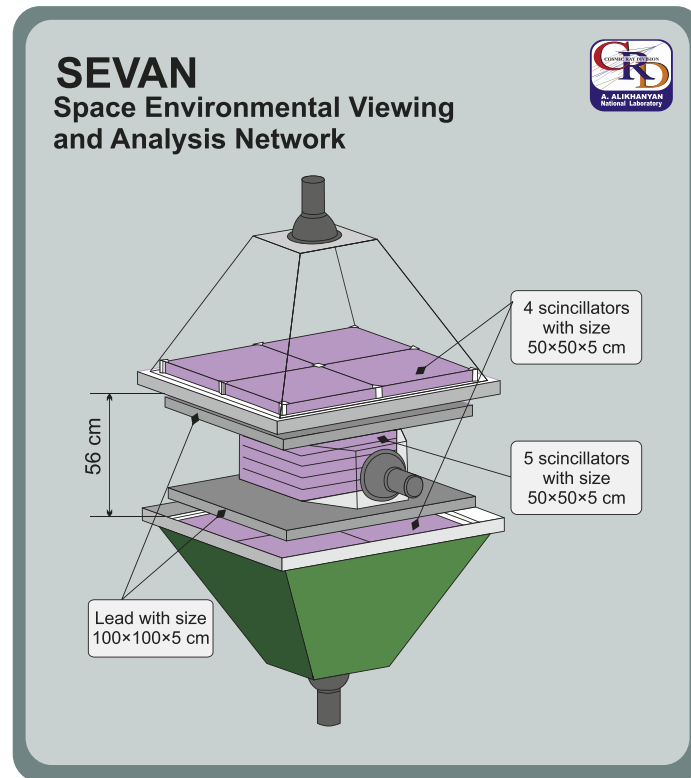


Fig. 2. A SEVAN particle detector.

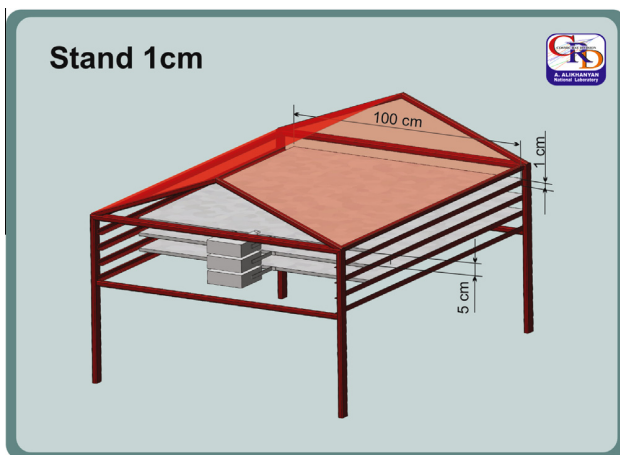


Fig. 3. STAND1 stacked detector.

Coincidentally, the particle fluxes observed by the network of NaI crystals and other particle detectors just beneath the cloud start to increase at 8:50, see Fig. 6. The figure does not show the time series of the count rates itself, but the time series of the p -values of the peak significance test. The p -value is the most comprehensive measure of the reliability of detecting peaks in a time series. Large p -value corresponds to small chance probabilities that the observed peak is a background fluctuation and not a genuine signal. Therefore, we can safely reject the null hypothesis (background fluctuation) and confirm the TGE. Very large p -values not only prove the unambiguous existence of a particle flux from the cloud, but also serve as a comparative measure of the TGE observations using different detectors. The largest p -value of 82σ

(standard deviations) is observed at 9:02 by the Aragats Multivariate Muon Monitor (AMMM), an array of 25 plastic scintillators with dimensions $100 \times 100 \times 1 \text{ cm}^3$ located outdoors in iron housings. The peak registered by the STAND1 detector at the same time has a p -value of $\sim 30 \sigma$, that of the CUBE detector of $\sim 22 \sigma$. The differences in p -values are due to various sizes and energy thresholds of detectors. Thus, the indoor CUBE detector with its higher energy threshold did not detect the small peak at

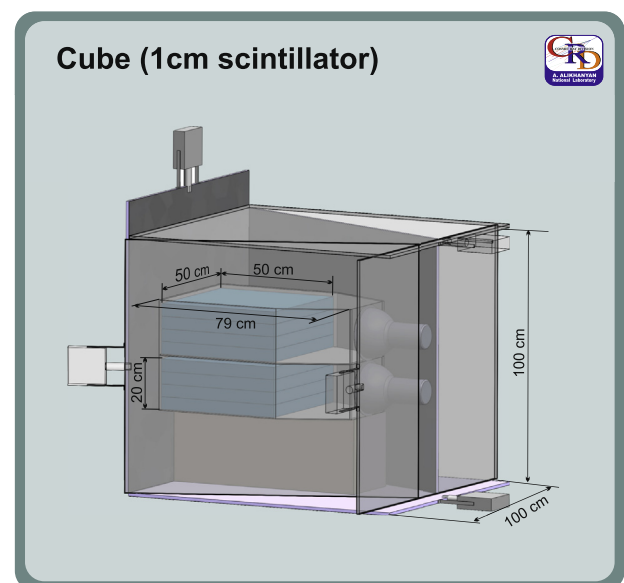


Fig. 4. The Cube detector with a veto against charged particles.

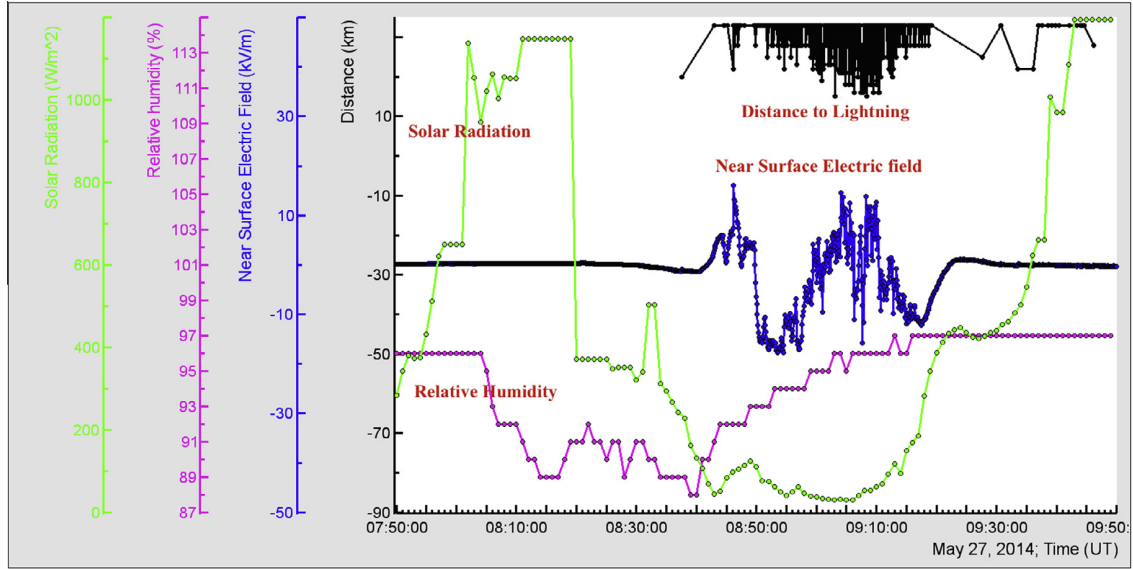


Fig. 5. Time series of the meteorological conditions (solar radiation, relative humidity, near-surface electric field) and the distance to the lightning during the TGE on May 27, 2014. The distance is measured using an electric mill EFM-100 (BOLTEK).

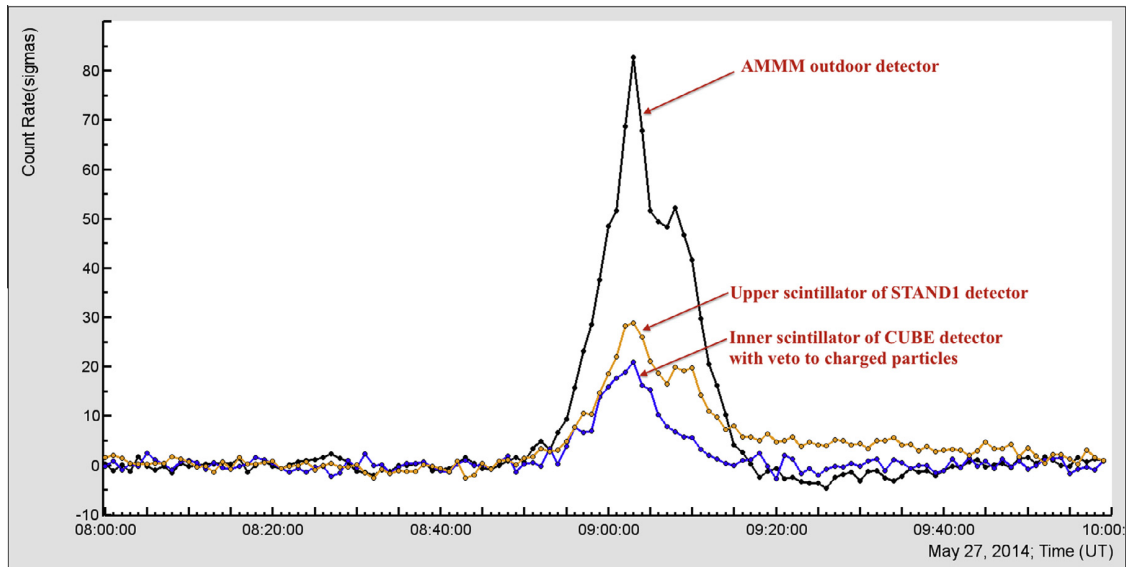


Fig. 6. One-minute time series of the significances of the measured peak values against the background-only hypothesis. (p -values of t -test).

9:08 seen by the outdoor detectors AMMM and STAND1. To reveal this enhancement in more details we present in Fig. 7 the one-second time series of the 3 cm thick outdoor plastic scintillator, apparently showing the second peak at 9:08.

The disturbance of the electric field finished at 9:23. According to the pattern of the electric field generated by three differently charged layers in the thundercloud, the lower two of which are responsible for the particle acceleration towards Earth. This TGE belongs to the 1st category of our classification (see [5]); after a few minutes in the positive domain the electric field changes polarity and mostly remains in the negative domain; simultaneously the particle flux abruptly increases.

The stacked detector assembly allows a rough estimate of the fraction of electrons in the particle flux of the TGE. The existence

of two neighboring peaks in the TGE allows the estimation of the electron contamination of the gamma ray flux.

From simulations and from calibration experiments¹ we estimate the efficiency of the STAND1 scintillators for charged particles as 98.5%. Consequently, the probability to miss a particle is 1.5%. Using the energy spectrum recovered by the NaI spectrometers network (see details in [7]) we estimate with the GEANT code the probability of registering a gamma ray during the 27 May TGE of the upper, middle and bottom layers of STAND1 detector to be 1.6%, 1.9% and 2.0%, respectively. Using these efficiencies we can

¹ For instance, by comparing “111” and “101” coincidences in the STAND1 detector (signals in all three layers and signals only in layers 1 and 3) and dividing N_{101}/N_{111} , we estimate the efficiency of electron detection to be $\sim 98.5\%$

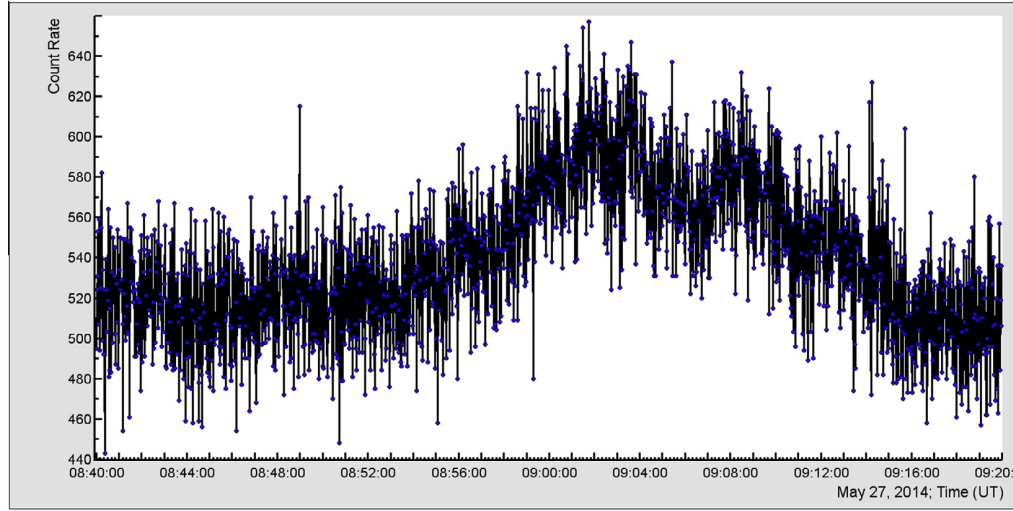


Fig. 7. 1-s time series of the stand-alone $100 \times 100 \times 3 \text{ cm}^3$ outdoor plastic scintillator.

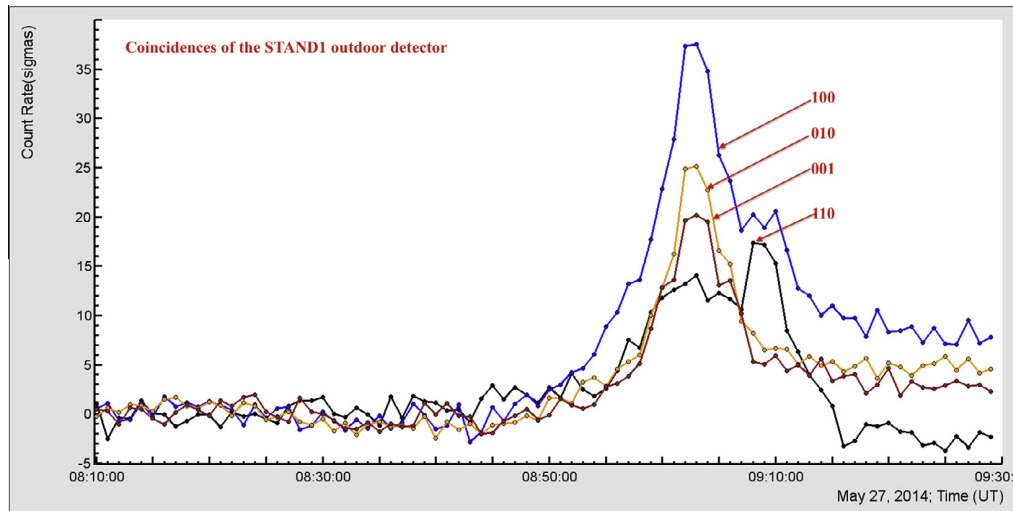


Fig. 8. One-minute time series of different codes of the 3-layered STAND1 detector (p -values).

easily calculate the conditional probabilities of each trigger condition to be originated by an electron or a gamma ray.

As we can see in Fig. 8, the “110” trigger pattern is the only one revealing a second peak at 9:08 larger than that at 9:02. In turn, the pattern “001” does not reveal any peak at 9:08. We estimate the probabilities that pattern “110” is due to gamma rays or electrons, respectively. The probability that a gamma ray is registered in two successive layers and not detected in the last one is only $\sim 3 \times 10^{-4}$. For an electron the probability of such a pattern is at least 50 times larger. Therefore, we can deduce that the trigger pattern “110” selects mostly electrons. The probability that an electron misses two successive layers and gives signal in the last one is only $\sim 2.2 \times 10^{-4}$, for gamma rays this probability is ~ 100 times larger. Therefore, we can deduce that the pattern “001” selects mostly gamma rays. This analysis demonstrates that the peak around 9:02 originates mostly from gamma rays and the peak at 9:08, is mainly due to electrons. At 9:01–9:03 the intensity of electrons is much lower than the intensity of gamma rays. Therefore, we can use this particular TGE for the calibration of the ASEC particle detectors. The differential energy spectrum of the particle flux

detected at 9:01–9:03 by all five NaI spectrometers along with the power-law fit parameters is depicted in Fig. 9.

4. Estimation of the “effective” energy thresholds of the ASEC detectors

According to the techniques described in the previous section we select five TGEs with a small fraction of electrons from all TGE events detected in 2013–2014. These are TGEs observed on May 12, 2013, on June 19, 2013, on July 9, 2013, on May 27, 2014 and on June 12, 2014. The joint sample of the energy releases detected during these TGEs was converted into energies of particles and an averaged integral energy spectrum was calculated. The same averaging procedure was used for the count rates of other particle detectors.

In Fig. 10 we depict the integral spectrum of gamma rays obtained with the NaI network along with counts (integral spectra) of several ASEC detectors, measured during the same time intervals.

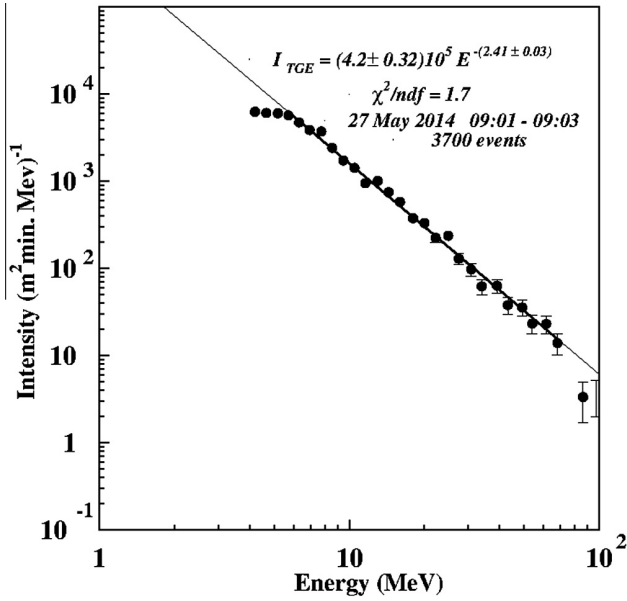


Fig. 9. The differential spectrum recorded with the five NaI crystal detectors between 9:01 and 9:03 at 27 May, 2014.

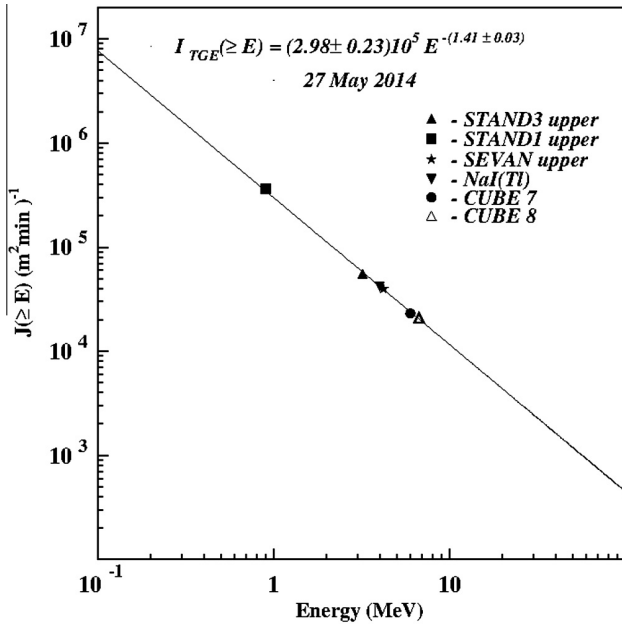


Fig. 10. The integral energy spectra of gamma rays with intensities measured with different ASEC particle detectors.

All of the ASEC detectors use scintillators or NaI crystals read out with photomultipliers. To avoid spurious low-amplitude pulses due to photomultiplier noise we use discriminators with predefined threshold values². However, particles with energies equal or near to this “electronic” energy threshold are not registered with 100% efficiency. The notion of the “physical” energy threshold is not firmly established. We can arbitrarily define the physical energy threshold of a detector as the energy at which the particles are

² Sometimes the electronics threshold is artificially enlarged to cut the low energy particle flux.

registered with 10%, 50%, 90% or even 99% efficiency. To avoid this arbitrariness we introduce the notion of “effective” energy threshold by simply comparing the detector count rate with the energy spectrum measured with the more precise spectrometers. As it is shown on Fig. 10 we simply place the value of the particular particle detector count rate on the y-axis of the integral energy spectrum. By reading the corresponding energy from the x-coordinate axis beneath, we obtain the “effective” threshold.

In Table 1 we compare the mean values of the “effective thresholds” obtained with five selected TGEs with a small fraction of electrons for several ASEC detectors. The fraction of electrons was estimated for all five events according to the statistical techniques described in the previous section. In the second column of Table 1 we show the “effective thresholds” obtained by reading the x-coordinate of Fig. 10 when the y-coordinate (intensity measured by particular detector) was placed on the integral gamma-ray energy spectrum. In the third column we list the previously estimated thresholds obtained from the measured CR background count rates showing the single-muon peak. The maximum intensity in the CR

Table 1

Effective energy threshold of ASEC detectors estimated by the mean flux of the five selected TGEs.

| Detector | Estimated “effective” energy threshold (MeV) | Estimated energy threshold based on CR background (MeV), “ADC count = 1” energy |
|--|--|---|
| CUBE inner 20-cm thick scintillator (upper) | 5.3 ± 0.6 | 5.8 ± 0.6 |
| CUBE inner 20-cm thick scintillator (bottom) | 5.4 ± 1.1 | 6.4 ± 0.6 |
| SEVAN upper 5-cm thick scintillator | 3.6 ± 0.6 | ^a |
| STAND1 upper 1-cm thick scintillator | 0.7 ± 0.1 | ^a |
| STAND 3 upper 3-cm thick scintillator | 2.9 ± 0.3 | 3.5 ± 0.4 |

^a SEVAN and STAND1 detectors measure only count rates and not energy releases as other ASEC detectors, therefore we cannot estimate their energy threshold using the muon peak.

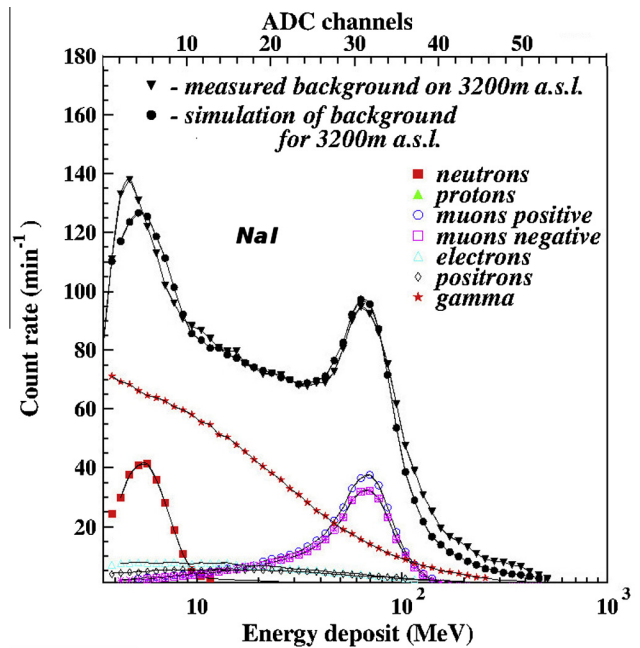


Fig. 11. Comparison of the simulated secondary cosmic ray flux on 3200 m height with the SCR flux measured by the NaI spectrometer.

background, the so-called muon peak, is used for the calibration of the energy deposit histogram by establishing the correspondence between ADC counts and energies in MeV.

In Fig. 11 we present the simulated background spectrum (in MeV) by calculating the response to almost all species of secondary cosmic rays. The simulated spectrum is compared with the experimentally measured spectrum of ADC counts, which gives the correspondence between the scales in energy and ADC counts. We know from simulations that the second peak in the background spectrum is due to the traversal of 60 MeV muons (corresponding to the most probable energy release in a 12 cm thick NaI crystal). The same peak in the spectrum measured with the NaI spectrometers is located near the ADC count 31. Thus the 31st ADC count corresponds to ~ 60 MeV and ADC count 1 (determining the energy threshold) to ~ 3.6 MeV.

5. Conclusions

We are continuously measuring energy spectra of gamma rays from thunderclouds, so called Thunderstorm Ground Enhancements, with the help of NaI crystals. We use these spectra to calibrate the plastic scintillation detectors of the Aragats Space Environmental Center. We introduced the notion of an “effective energy threshold” which permits to avoid the arbitrariness of the previously used method of the estimation of the energy corresponding to the first ADC count. Our method is also applicable to particle detectors measuring only the count rate and not the spectra of the deposited energy. It can be used for the multi-year monitoring of the characteristics of large arrays of particle detectors registering fluxes of secondary cosmic rays.

Acknowledgments

The authors are grateful to the staff of Aragats research high-altitude station of the Yerevan Physics Institute for the

uninterrupted operation of the ASEC facilities, and to participants of the seminar of the Cosmic Ray Division for useful discussions.

A.C. and S.C. are grateful to Harutun Vaporciyan for support.

Christian Spiering’s suggestions have highly improved the quality of the paper, author greatly appreciate his time and efforts.

References

- [1] S. Agostinelli, J. Allison, K. Amako, et al., GEANT4 – a simulation toolkit, *Nucl. Instrum. Methods A* 506 (2003) 250.
- [2] A. Chilingarian, K. Arakelyan, K. Avakyan, et al., Correlated measurements of secondary cosmic ray fluxes by the Aragats space-environmental center monitors, *Nucl. Instrum. Methods A* 543 (2–3) (2005) 483.
- [3] A. Chilingarian, A. Daryan, K. Arakelyan, et al., Ground-based observations of thunderstorm-correlated fluxes of high-energy electrons, gamma rays, and neutrons, *Phys. Rev. D* 82 (2010) 043009.
- [4] A. Chilingarian, G. Hovsepyan, A. Hovhannisyan, Particle bursts from thunderclouds: natural particle accelerators above our heads, *Phys. Rev. D* 83 (2011) 062001.
- [5] A. Chilingarian, H. Mkrtchyan, Role of the lower positive charge region (LPCR) in initiation of the thunderstorm ground enhancements (TGEs), *Phys. Rev. D* 86 (2012) 072003.
- [6] A. Chilingarian, L. Vanyan, B. Mailyan, Observation of thunderstorm ground enhancements with intense fluxes of high-energy electrons, *Astropart. Phys.* 48 (2013) 1.
- [7] A. Chilingarian, H. Hovsepyan, L. Kozliner, Thunderstorm ground enhancements – gamma ray differential energy spectra, *Phys. Rev. D* 88 (2013) 073001.
- [8] A. Chilingarian, Thunderstorm ground enhancements – model and relation to lightning flashes, *J. Atmos. Solar-Terr. Phys.* 107 (2014) 68.
- [9] J.R. Dwyer, D.M. Smith, S.A. Cummer, High-energy atmospheric physics: terrestrial gamma-ray flashes and related phenomena, *Space Sci. Rev.* 173 (2012) 133.
- [10] J.R. Dwyer, M.A. Uman, The physics of lightning, *Phys. Rep.* 534 (2014) 147.
- [11] A.V. Gurevich, A.N. Karashtin, Runaway breakdown and hydrometeors in lightning initiation, *Phys. Rev. Lett.* 110 (2013) 185005.
- [12] T. Shibata, M. Beitollahi, M. Fukushima, For the telescope array collaboration absolute energy calibration of the telescope array fluorescence detector with an electron linear accelerator, *EPJ Web Conf.* 53 (2013) 10004.